

Published in J Vet Intern Med 2011;25:330-338

DOI 10.1111/j.1939-1676.2010.0663.x

Quantification of left ventricular longitudinal strain, strain rate, velocity and displacement in healthy horses by two-dimensional speckle tracking

Decloedt Annelies, Verheyen Tinne, Sys Stanislas, De Clercq Dominique, van Loon Gunther

Department of Large Animal Internal Medicine, Faculty of Veterinary Medicine, Ghent University, Belgium

Short title: LV longitudinal function by 2DST

Keywords: cardiology, echocardiography, myocardial function, 2D strain, contractility

Abbreviations

2DST, two-dimensional speckle tracking

AVC_a, time of aortic valve closure automatically calculated by the software

AVC_{MM}, time of aortic valve closure measured by M-mode

bpm, beats per minute

DL_S, peak systolic longitudinal displacement

fps, frames per second

HR, heart rate

LV, left ventricle

ROI, region of interest

SL_G, peak maximal longitudinal strain

SL_P, peak positive longitudinal strain

SL_S, peak systolic longitudinal strain

SrL_A, peak late diastolic longitudinal strain rate

SrL_E, peak early diastolic longitudinal strain rate

SrL_S, peak systolic longitudinal strain rate

TDI, tissue Doppler imaging

VL_A, peak late diastolic longitudinal velocity

VL_E, peak early diastolic longitudinal velocity

VL_S, peak systolic longitudinal velocity

Corresponding author: Decloedt Annelies, Department of Large Animal Internal Medicine, Faculty of Veterinary Medicine, Ghent University, Salisburylaan 133, 9820 Merelbeke, Belgium, annelies.decloedt@ugent.be

This study was carried out at the Department of Large Animal Internal Medicine, Faculty of Veterinary Medicine, Ghent University, Belgium

Acknowledgements: Annelies Decloedt is a PhD fellow of the Research Foundation - Flanders (FWO).

Part of this work has been presented at the 48th BEVA Congress, Birmingham, UK, September 9-12, 2009.

ABSTRACT

Background: The quantification of equine left ventricular (LV) function is generally limited to short-axis M-mode measurements. However, LV deformation is three-dimensional and consists of longitudinal shortening, circumferential shortening and radial thickening. In human medicine, longitudinal motion is the best marker of subtle myocardial dysfunction.

Objectives: To evaluate the feasibility and reliability of two-dimensional speckle tracking (2DST) for quantifying equine LV longitudinal function.

Animals: Ten healthy untrained trotter horses; 9.6 ± 4.4 years; 509 ± 58 kg.

Methods: Prospective study. Repeated echocardiographic examinations were performed by two observers from a modified four-chamber view. Global, segmental and averaged peak values and timing of longitudinal strain (SL), strain rate (SrL), velocity (VL) and displacement (DL) were measured in four LV wall segments. The inter- and intra-observer within- and between-day variability was assessed by calculating the coefficients of variation for repeated measurements.

Results: 2DST analysis was feasible in each exam. The variability of peak systolic values and peak timing was low to moderate, whereas peak diastolic values showed a higher variability. Significant segmental differences were demonstrated. DL and VL presented a prominent base-to-midwall gradient. SL and SrL values were similar in all segments except the basal septal segment, which showed a significantly lower peak SL occurring about 60 ms later compared to the other segments.

Conclusions and clinical importance: 2DST is a reliable technique for measuring systolic LV longitudinal motion in healthy horses. This study provides preliminary reference values which can be used when evaluating the technique in a clinical setting.

INTRODUCTION

The quantification of myocardial function is important in horses, particularly in cases of poor performance. The objective evaluation of left ventricular (LV) function is traditionally based on M-mode measurements such as fractional shortening and wall thickening.^{1,2} These measurements provide a rather rough estimate of global LV function, as they are focal and one-dimensional. Recently, new techniques have been introduced in equine cardiology that require further investigation. Tissue Doppler imaging (TDI) has been used to measure the systolic and diastolic velocities of the myocardial walls.³⁻⁵ However, these measurements are easily influenced by the insonation angle and total heart motion. This limitation has led to a growing interest in strain imaging in human medicine. Strain is a measure of the amount of deformation of the myocardial walls, expressed in %. Lengthening or thickening is indicated by a positive strain value, while shortening or thinning is negative. The rate of deformation is the strain rate, expressed in s^{-1} . TDI-based strain imaging is slightly less angle-dependent compared to velocity measurements.

Two-dimensional speckle tracking (2DST) is not angle-dependent and allows quantification of myocardial strain in the two dimensions of the ultrasound image based on tracking speckles in the myocardial walls.^{6,7} 2DST has been reliably applied in short-axis images for quantification of equine radial and circumferential LV motion.⁸ However, LV contraction is a three-dimensional movement consisting of radial thickening, circumferential shortening and longitudinal shortening. In human medicine, longitudinal function is described as the best prognostic factor in several conditions such as valvular disease.⁹⁻¹¹ Although 2DST has recently been applied to measure equine LV longitudinal function during stress-echocardiography, no data are available on the reliability of these measurements.¹²

The purpose of our study was to assess global and regional LV longitudinal function in healthy horses at rest. We hypothesized that 2DST methods allow quantification of LV longitudinal strain, strain rate, velocity and displacement based on 2D greyscale images. The 2DST technique and the feasibility and reliability of the evaluation of equine LV longitudinal function are described.

MATERIAL & METHODS

Study Population: The study population consisted of ten healthy untrained trotter horses (seven mares, three geldings) aged 9.6 ± 4.4 years (mean \pm SD) with a body weight of 509 ± 58 kg. Animal handling and care was performed following the guidelines of the local ethical committee. A comprehensive examination was performed prior to the study to exclude cardiovascular or respiratory disease. This consisted of a general physical examination, thorough cardiac auscultation, 30 minute electrocardiogram at rest and routine 2D, M-mode and color Doppler echocardiography.

Echocardiography: All horses were examined without sedation at heart rates below 45 beats per minute (bpm). Echocardiography was performed using an ultrasound unit^a with phased array transducer^b at a frequency of 1.6/3.2 MHz (octave harmonics). A base-apex ECG was recorded simultaneously. At least three non-consecutive cardiac cycles from each view were stored in cine loop format.

M-mode recordings of the aortic valve were made in the right parasternal LV outflow tract long-axis view. For the evaluation of LV longitudinal function, a standard right parasternal four-chamber view¹ was obtained. The imaging depth ranged from 26 to 28 cm depending on LV size, with a single focus positioned at 20 cm. The sector width was reduced to 55° in order to achieve a frame rate of at least 40 frames per second (fps). The view was then slightly modified to include as much of the LV as possible while the mitral annulus remained visible throughout the entire cardiac cycle. As a result, the apex was not always visualized (Fig. 1).

Off-line analysis: Measurements were performed using a commercially available software package.^c For each exam, three non-consecutive cardiac cycles per view were analyzed one by one and the three measurements were averaged for all further analyses. The time of aortic valve closure (AVC_{MM}) was measured manually as the time interval between the R-wave on the ECG and aortic valve closure in the M-mode image. The RR interval was recorded and instantaneous heart rate was calculated as 60,000/RR interval.

LV longitudinal function was assessed from the modified four-chamber view with the “2D Strain” application, using the “4CH” mode. A U-shaped region of interest (ROI) was placed on the myocardium in a frame at end-systole by tracing the endocardial border from the septal to the lateral wall insertion of the mitral valve, without following excessive bulging of the walls. This line was partially drawn outside the image where the apical endocardial border was expected. Afterwards, the ROI width was adjusted in order to cover the entire myocardium without including the epicardial borders. The software algorithm subdivided this ROI into six segments (Fig. 1). The apical segments were excluded from further analysis as these segments were not visualised. The midwall segments were manually corrected if they did not fit the image width. Next, the program automatically selected acoustic speckles that were tracked throughout the cardiac cycle in longitudinal and transverse (radial) direction. Based on the tracking quality, the software approved or rejected the segments for further analysis. In addition, tracking quality was evaluated by visual assessment during motion playback. If necessary, the ROI was adjusted and tracking was repeated until adequate tracking quality was achieved. Segments were excluded if they were rejected by the software or if tracking was visually insufficient. If tracking was visually accurate during systole but not during diastole, only systolic measurements were included for further analysis. Occasionally the last systolic frames were poorly tracked in some segments. As the effect of one or two poorly tracked frames was thought to be minimal, these segments were included for further analysis. However, this might have resulted in a small underestimation of strain values in these segments.

After tracking quality had been verified for all segments, the trace analysis screen was shown. The following curves were displayed: longitudinal velocity (VL), strain (SL), strain rate (SrL) and displacement (DL), and transverse displacement (DT). The default settings for spatial smoothing, temporal smoothing and drift compensation were used. The time of aortic valve closure (AVC_a) was calculated by the software based on the longitudinal strain curves of all LV segments. Segmental systolic (s), early diastolic (e) and late diastolic (a) peak values were indicated on the curves and could be manually adjusted if necessary. Global and averaged peak values were determined as measurements of global LV function. Global values were computed by the software from the whole ROI as a single segment. These values were not

visible in the trace analysis screen but were included when all data were exported from the software. Averaged values were calculated manually for all measurements as the average of the segmental values. Furthermore, a distinction was made between peak systolic (SL_S) and maximal (SL_G) strain. SL_S and SL_G were the same if only one peak was present in the longitudinal strain curve, occurring before AVC_a . If the curve showed two peaks with the second and highest peak after AVC_a , this peak was considered SL_G and the peak before AVC_a was SL_S . If only one peak was present, occurring after AVC_a , the strain value at the time of aortic valve closure was considered SL_S while the peak after AVC_a was SL_G .

Reliability of Echocardiographic Variables: The reliability of all 2DST measurements was evaluated by comparing repeated echocardiographic examinations and off-line measurements performed by two experienced echocardiographers (AD and GVL). In total, thirty exams were performed. All horses were examined by observer 1 (AD) on two separate days with an interval of one day. On one of these occasions (day 1 in five horses and day 2 in five horses), the echocardiographic examination was repeated by observer 2 (GVL) immediately before (five horses) or after (five horses) the first observer. The off-line analysis was first performed by observer 1 for all echocardiographic exams ($n = 30$). Next, one exam of each horse was measured by both observers on a second, separate occasion to determine measurement variability ($n = 10$). At any time during off-line analysis, both observers were blinded to echocardiographer, horse, day and any previous results.

Statistical analysis: Statistical analyses were performed using dedicated computer software.^d Within- and between-day intra- and interobserver variability were determined based on the analysis of variance results of all measurements. The within-day interobserver variability was obtained by comparing the results of the exams performed on the same day by observer 1 and observer 2. The numerical values for the reported coefficients of variation (CV) were derived from the expressions of the expected mean square errors from a two-factor (observer and horse) analysis of variance of the natural logarithms of the measurements. In analogy, the between-day intra-observer variability was determined by comparing the exams recorded on two separate days by observer 1 using a two-factor (day and horse) analysis of variance. Similarly, the measurement variability was obtained by repeated measurements of thirty identical cycles (one exam per horse) on two different days (intra-observer measurement variability) or by two different observers (interobserver measurement variability). The degree of variability was defined based on the CV as follows: $CV < 15\%$, low variability; $CV 15\text{--}25\%$, moderate variability; $CV > 25\%$, high variability.¹³

Summary statistics for the different measurements (mean \pm SD; $n = 10$ horses) were calculated using the average measurement of three non-consecutive cycles per horse. Peak values and timing in the different segments were compared by analysis of variance; post-hoc tests were performed using the Bonferroni correction method. These data were displayed as box plots, with the box span indicating the middle half of the observations, the line in the box marking the median, and the whiskers indicating the range of observations. Extreme values were plotted individually at the end of the whiskers. Agreement between AVC_a and AVC_{MM} was assessed by Bland-Altman 95% limits of agreement. A paired t-test was used to compare both measurements of AVC and their corresponding heart rate, as well as to compare global and averaged values of SL and SrL. The level of significance was $\alpha = 0.05$.

RESULTS

2DST analysis was feasible on three cycles of each exam using the modified four-chamber view at a frame rate of 41.1 fps. Fig. 2A-E shows an example of the curves displayed by the software after approval of tracking quality. The shape of these curves was similar in all horses and peak values could be easily distinguished. All apical segments were excluded as they were not visualized. Tracking quality was approved in 574 of the remaining 600 segments (95.7%). However, the tracking process was visually less accurate in diastole. In 6.1% of the approved segments, tracking was very poor and diastolic values were excluded from further analysis. Tracking quality of transverse motion was often visually inadequate and the variability of the measurements was very high ($CV > 25\%$). Therefore these measurements are not further discussed.

Tables 1 and 2 show the peak values of global, averaged and segmental 2DST measurements in the study population. The global SL_G value was not significantly different from the averaged SL_G ($P = 0.055$). The global SrL values were slightly lower than the averaged SrL values ($P < 0.001$). Significant segmental differences were found. As illustrated in Fig. 3A-B, DL and VL presented a remarkable base-to-midwall gradient ($P < 0.001$). Conversely, SL and SrL values were similar in all segments except the basal septal segment (Fig. 3C-D). This segment showed a significantly less negative SL_S ($P < 0.001$) and SL_G ($P = 0.022$).

The mean AVC_a was 528 ms, which did not differ significantly from the AVC_{MM} of 537 ms ($P = 0.070$). A mean bias of -10 ms with a standard deviation of 14 ms was present, resulting in 95% limits of agreement between -36 and + 18 ms. The mean RR interval of 2DST and M-mode recordings did not differ significantly ($P = 0.35$).

The mean values of peak timing are provided in Supplementary Table 1. Some remarkable segmental differences were present. SL_G was reached significantly later in the basal septal segment compared to the other segments ($P < 0.001$) (Fig. 3E). The mean delay of this segment was 60 ms (95% confidence interval 37 to 84 ms). Consequently, SL_G occurred after AVC_a in 107 of the 139 basal septal segments and in only 74 of the 435 other segments. At the onset of systole, 96% of the analysed basal septal segments showed a small positive peak strain (SL_P), compared to only 35% of the other segments. Time to peak VL_A and SrL_A was significantly delayed in the lateral wall compared to the septum ($P < 0.001$) (Fig. 3F). The difference of means for VL_A and SrL_A was 31 ms (95% confidence interval 20 to 41 ms) and 25 ms (95% confidence interval 16 to 34 ms) respectively.

Reliability: As shown in Tables 1 and 2, the variability of segmental, global and averaged peak systolic values was low to moderate, whereas diastolic measurements showed a moderate to high variability. SL and SrL exhibited a lower variability than VL and DL. Conversely, the variability of SL_P was very high (CV 58 - 226%). The variability of peak timing was low, except for time to peak VL_S , SrL_S and SL_P , which showed a moderate to high variability (Supplementary Table 1).

DISCUSSION

This study describes the technique and demonstrates the feasibility of quantifying LV longitudinal function by 2DST in healthy horses at rest. Global and regional systolic myocardial strain, strain rate, velocity and displacement could be reliably measured using a modified right parasternal four-chamber view.

The technique of 2DST is based on tracking the movement of acoustic speckles in the 2D greyscale image from one frame to another. An appropriate frame rate is a prerequisite for adequate 2DST-analysis. A frame rate of 41.1 fps was used, which is within the range of frame rates applied in human medicine (30 to 90 fps)^{14,15} and recommended by the software manufacturer (40 to 70 fps).^c Lower frame rates result in large frame-to-frame changes in speckle position and a decreased time resolution. This causes impaired tracking quality and underestimation of peak values, especially at increased heart rates.⁶ In this study, a sufficient frame rate was obtained by limiting the image width to 55°, which did not allow visualizing the entire LV throughout the cardiac cycle. The basal and midwall segments were chosen for analysis as these show the largest longitudinal movement. The frame rate was not increased by reducing the line density of the ultrasound beams, as this results in a decreased lateral resolution. Adequate lateral resolution is important for tracking quality, especially when measuring longitudinal strain from a right parasternal four-chamber view. The use of more advanced echocardiographic equipment and transducers may result in an improved lateral resolution, thus enabling the acquisition of higher frame rates at a wider imaging sector.

As 2DST is a new technique, a thorough evaluation of repeatability and reproducibility is crucial before clinical use. All systolic peak values showed a low to moderate between-day and interobserver acquisition and measurement variability and can thus be reliably investigated in future clinical studies. Our reliability data are similar to those reported for 2DST in human medicine, small animals and horses.^{8,16-18} However, it should be noted that the comparison of different reliability studies is difficult due to different sample size and statistical methods for assessment of reliability. In our study, diastolic measurements were less reliable as tracking was often visually inaccurate in early diastole because of the fast cardiac movement in this phase. Due to the relatively low frame rate, this early diastolic peak was underestimated by 2DST and early and late diastolic values were approximately equal. In reality, the early diastolic peak is probably much higher than the late diastolic peak in horses at rest, as has already been demonstrated for radial diastolic wall motion velocities by TDI.⁵

2DST analysis of longitudinal function was feasible in all exams, although 4.3% of segments were excluded because of inadequate tracking quality. Similarly, 5/90 segments were excluded at resting heart rate in a previous study on equine LV longitudinal function by 2DST.¹² The percentage of excluded segments in human medicine ranges from 2.2 to 20% in healthy and diseased study populations.^{15,19,20} In our study, the basal segments were most frequently excluded. It is important to note that some loops contained artefacts in the mitral annular region. Strict guidelines on the image quality in this region will lead to a lower number of excluded segments. Attention should be paid to an optimal gain and contrast for imaging the myocardium, thereby reducing artefacts. It is particularly important to avoid the presence of drop-out due to the ribs or the coronary region. Furthermore, the mitral annular

ring has to remain visualised throughout the entire cardiac cycle, also during atrial contraction.

One of the main goals of our study was the quantification of global LV longitudinal function. For this purpose global and averaged peak values were evaluated. Although there was a trend for global SL_G to be lower than averaged SL_G , the difference was small (mean bias -0.5%) and statistically insignificant. Global SrL values were 5-16% lower compared to the averaged SrL values. Global and averaged SL_G and SrL_S measurements were equally reliable. However, global values are computed automatically while averaged values need to be calculated manually. Therefore global SL and SrL values are more attractive to be used in a clinical setting. VL and DL are less applicable as measurements of global LV function due to large segmental differences. Because of the fixed position of the apex in the thorax, the mitral annular ring is pulled down towards the apex during systole. As a result, longitudinal velocity and displacement are largest in segments further away from the apex. The downward motion of the LV base not only results in ejection of blood from the ventricle, but also in passive filling of the atria. The longitudinal base-to-apex gradient is also present in man and small animals.²⁰⁻²² SL and SrL values did not show this gradient, indicating that all segments shorten almost equally. However, peak SL was significantly lower in the basal septal segment. The basal septal regions also exhibited the lowest contractile indices in the canine and human normal LV.^{17,23}

Our results demonstrated significant segmental differences of peak timing. Although there was a trend of AVC_a to occur earlier than AVC_{MM} , the difference was clinically irrelevant (mean bias -10 ms) and statistically insignificant. AVC_a was thus considered the end of systole. Postsystolic motion, defined as SL_G occurring after AVC_a , was present in 31% of segments. This is comparable to human medicine, where postsystolic motion is recorded in about 30% of myocardial segments in healthy people.²⁴ The clinical relevance of the observed postsystolic motion in supposedly healthy horses requires further investigation. However, postsystolic shortening was predominantly observed in the basal septal segment. In the normal human LV, peak strain was also found to be 35 to 55 ms delayed in the basal septum, which is probably caused by a delayed activation of this segment.^{25,26} This hypothesis is supported by the frequent presence of early systolic SL_P in the basal septal segments in our study. This lengthening of the myocardium arises when a delayed activated segment is passively stretched while the other segments start to contract. In the basal septal segment, a small SL_P can be considered as normal. In healthy horses, the variability of SL_P measurements was very high due to the low peak values. However, the presence of a high SL_P in other segments than the basal septal might be useful in a clinical setting as a measure of dyssynchrony.

Surprisingly, a small but significant delay of VL_A and SrL_A in the LV free wall was found. This might be caused by a delayed activation of the left atrium. Due to the location of the sinoatrial node, the right atrium is depolarized before the left atrium. The septum and right ventricular free wall are stretched at the time of right atrial contraction, while stretching of the lateral wall is caused by the subsequent contraction of the left atrium.

The clinical value of LV longitudinal function is extensively documented in human medicine. Several studies have demonstrated that longitudinal function is a sensitive marker for impaired LV function.⁹⁻¹¹ In asymptomatic patients with mitral valve disease, myocardial

dysfunction can be detected by a decrease in longitudinal shortening. This systolic dysfunction is present before changes in conventional echocardiographic measurements occur. The underlying mechanism is the high vulnerability of the subendocardial longitudinal fibres, whereas the circumferential fibres are less prone to myocardial damage and compensate for the loss of longitudinal function.²⁷ Further studies are required to evaluate if equine LV longitudinal function is also altered by valvular regurgitation. As of yet, the only studies on the use of 2DST in equine cardiology were conducted on healthy adult horses at rest and after exercise.^{8,12} SL_G , SrL_S , DL_S and time to peak SL_G have been used to quantify LV longitudinal function. At resting heart rates, peak values and timing were similar to those reported in our study. Significant alterations were demonstrated during post-exercise stress echocardiography. However, it remains to be determined whether 2DST measurements can be used to detect stress-induced hypokinesia, akinesia or LV dyssynchrony.

The main limitations of our study were inherent to the 2DST technique. An adequate image quality is a prerequisite for accurate tracking. Artefacts such as reverberations and drop-out should be avoided during image acquisition, as they have a detrimental effect on the tracking quality. A thorough visual assessment of image quality is recommended before starting off-line analysis. A more hidden drawback of 2DST is the extensive smoothing of the curves. This might result in normally appearing curves even when visual tracking quality is poor. For this reason, visual evaluation of tracking quality is indispensable and should be performed before approving any results.

Measurements of longitudinal function were not compared to a gold standard, as there is no such technique available in horses. However, 2DST has been extensively validated in vitro, in animal models and in man, using sonomicrometry and MRI.^{19,28,29} Therefore it can be assumed that the 2DST measurements are closely correlated to the actual deformation of the equine ventricular walls. It should be noted that our results may only be valid for 2DST analyses using the same ultrasound machine, transducer and off-line analysis software and settings.

Our study was performed on ten horses. A larger study population would have allowed to establish more accurate reference values and to identify influences of body weight, height, breed, sex and training. This was beyond the scope of this study. Nevertheless, based on our results, preliminary reference values for healthy horses could be formulated.

In conclusion, 2DST was found to be a reliable technique for measuring left ventricular systolic longitudinal strain, strain rate, velocity and displacement. These measurements offer new insights into equine ventricular motion and enable a more complete quantification of myocardial function. Further research should be performed in a larger population of healthy and diseased horses to evaluate the value of this technique in horses with cardiac disease.

FOOTNOTES

^a GE Vivid 7 Dimension, GE Healthcare, Horten, Norway

^b 3S Phased Array Transducer, GE Healthcare, Horten, Norway

^c EchoPAC Software Version 7.1.2, GE Healthcare, Horten, Norway

^d SPSS Statistics 17.0, Rel. 17.0.1. 2008, Chicago: SPSS Inc

REFERENCES

1. Long KJ, Bonagura JD, Darke PG. Standardised imaging technique for guided M-mode and Doppler echocardiography in the horse. *Equine Vet J* 1992;24:226-235.
2. Patteson MW, Gibbs C, Wotton PR, et al. Echocardiographic measurements of cardiac dimensions and indices of cardiac function in normal adult thoroughbred horses. *Equine Vet J Suppl* 1995;19:18-27.
3. Sepulveda MF, Perkins JD, Bowen IM, et al. Demonstration of regional differences in equine ventricular myocardial velocity in normal 2-year-old thoroughbreds with Doppler tissue imaging. *Equine Veterinary Journal* 2005;37:222-226.
4. Gehlen H, Iversen C, Stadler P. Tissue Doppler echocardiographic examinations at rest and after exercise in horses with atrial fibrillation. *Pferdeheilkunde* 2009;25:11-16.
5. Schwarzwald CC, Schober KE, Bonagura JD. Methods and reliability of tissue Doppler imaging for assessment of left ventricular radial wall motion in horses. *J Vet Intern Med* 2009;23:643-652.
6. Teske AJ, De Boeck BW, Melman PG, et al. Echocardiographic quantification of myocardial function using tissue deformation imaging, a guide to image acquisition and analysis using tissue Doppler and speckle tracking. *Cardiovasc Ultrasound* 2007;5:27-45.
7. D'Hooge J, Heimdal A, Jamal F, et al. Regional strain and strain rate measurements by cardiac ultrasound: principles, implementation and limitations. *Eur J Echocardiogr* 2000;1:154-170.
8. Schwarzwald CC, Schober KE, Berli AS, et al. Left ventricular radial and circumferential wall motion analysis in horses using strain, strain rate, and displacement by 2D speckle tracking. *J Vet Intern Med* 2009;23:890-900.
9. Lancellotti P, Cosyns B, Zacharakis D, et al. Importance of left ventricular longitudinal function and functional reserve in patients with degenerative mitral regurgitation: assessment by two-dimensional speckle tracking. *J Am Soc Echocardiogr* 2008;21:1331-1336.
10. Mizuguchi Y, Oishi Y, Miyoshi H, et al. The functional role of longitudinal, circumferential, and radial myocardial deformation for regulating the early impairment of left ventricular contraction and relaxation in patients with cardiovascular risk factors: A study with two-dimensional strain imaging. *J Am Soc Echocardiogr* 2008;21:1138-1144.
11. Marciniak A, Sutherland GR, Marciniak M, et al. Myocardial deformation abnormalities in patients with aortic regurgitation: a strain rate imaging study. *Eur J Echocardiogr* 2009;10:112-119.
12. Schefer KD, Bitschnau C, Weishaupt MA, et al. Quantitative Analysis of Stress Echocardiograms in Healthy Horses with 2-Dimensional (2D) Echocardiography, Anatomical M-Mode, Tissue Doppler Imaging, and 2D Speckle Tracking. *J Vet Intern Med* 2010;24:918-931.
13. Schwarzwald CC, Schober KE, Bonagura JD. Methods and reliability of echocardiographic assessment of left atrial size and mechanical function in horses. *Am J Vet Res* 2007;68:735-747.
14. D'Hooge J, Bijnen B. The principles of ultrasound based motion and deformation estimation. In: Sutherland GR, Hatle L, Claus P, eds. *Doppler myocardial imaging : a textbook*, 1st ed. Hasselt, Belgium: BSWK; 2006:23-48.

15. Suffoletto MS, Dohi K, Cannesson M, et al. Novel speckle-tracking radial strain from routine black-and-white echocardiographic images to quantify dyssynchrony and predict response to cardiac resynchronization therapy. *Circulation* 2006;113:960-968.
16. Chetboul V, Serres F, Gouni V, et al. Radial strain and strain rate by two-dimensional speckle tracking echocardiography and the tissue velocity based technique in the dog. *J Vet Cardiol* 2007;9:69-81.
17. Hurlburt HM, Aurigemma GP, Hill JC, et al. Direct ultrasound measurement of longitudinal, circumferential, and radial strain using 2-dimensional strain imaging in normal adults. *Echocardiography* 2007;24:723-731.
18. Thorstensen A, Dalen H, Amundsen BH, et al. Reproducibility in echocardiographic assessment of the left ventricular global and regional function, the HUNT study. *Eur J Echocardiogr* 2010;11:149-156.
19. Amundsen BH, Helle-Valle T, Edvardsen T, et al. Noninvasive myocardial strain measurement by speckle tracking echocardiography: validation against sonomicrometry and tagged magnetic resonance imaging. *J Am Coll Cardiol* 2006;47:789-793.
20. Leitman M, Lysyansky P, Sidenko S, et al. Two-dimensional strain - A novel software for real-time quantitative echocardiographic assessment of myocardial function. *J Am Soc Echocardiogr* 2004;17:1021-1029.
21. Chetboul V, Sampedrano CC, Gouni V, et al. Ultrasonographic assessment of regional radial and longitudinal systolic function in healthy awake dogs. *J Vet Intern Med* 2006;20:885-893.
22. Chetboul V, Sampedrano CC, Tissier R, et al. Quantitative assessment of velocities of the annulus of the left atrioventricular valve and left ventricular free wall in healthy cats by use of two-dimensional color tissue Doppler imaging. *Am J Vet Res* 2006;67:250-258.
23. Haendchen RV, Wyatt HL, Maurer G, et al. Quantitation of regional cardiac function by two-dimensional echocardiography. I. Patterns of contraction in the normal left ventricle. *Circulation* 1983;67:1234-1245.
24. Voigt JU, Lindenmeier G, Exner B, et al. Incidence and characteristics of segmental postsystolic longitudinal shortening in normal, acutely ischemic, and scarred myocardium. *J Am Soc Echocardiogr* 2003;16:415-423.
25. Kowalski M, Kukulski T, Jamal F, et al. Can natural strain and strain rate quantify regional myocardial deformation? A study in healthy subjects. *Ultrasound Med Biol* 2001;27:1087-1097.
26. Sengupta PP, Krishnamoorthy VK, Korinek J, et al. Left ventricular form and function revisited: Applied translational science to cardiovascular ultrasound imaging. *J Am Soc Echocardiogr* 2007;20:539-551.
27. Lee R, Hanekom L, Marwick TH, et al. Prediction of subclinical left ventricular dysfunction with strain rate imaging in patients with asymptomatic severe mitral regurgitation. *Am J Cardiol* 2004;94:1333-1337.
28. Sivesgaard K, Christensen SD, Nygaard H, et al. Speckle tracking ultrasound is independent of insonation angle and gain: an in vitro investigation of agreement with sonomicrometry. *J Am Soc Echocardiogr* 2009;22:852-858.

29. Korinek J, Wang J, Sengupta PP, et al. Two-dimensional strain--a Doppler-independent ultrasound method for quantitation of regional deformation: validation in vitro and in vivo. J Am Soc Echocardiogr 2005;18:1247-1253.

FIGURES

Figure 1: Modified four-chamber view for 2DST analysis of LV longitudinal function. The ROI is automatically divided into six segments: “basSept”, “midSept” and “apSept” for the interventricular septum; “basLat”, “midLat” and “apLat” for the LV free wall. Tracking quality is verified by the software and displayed at the bottom of the screen. Approved segments are marked with a green “V”. The apical segments are rejected, as indicated by a red “X”.

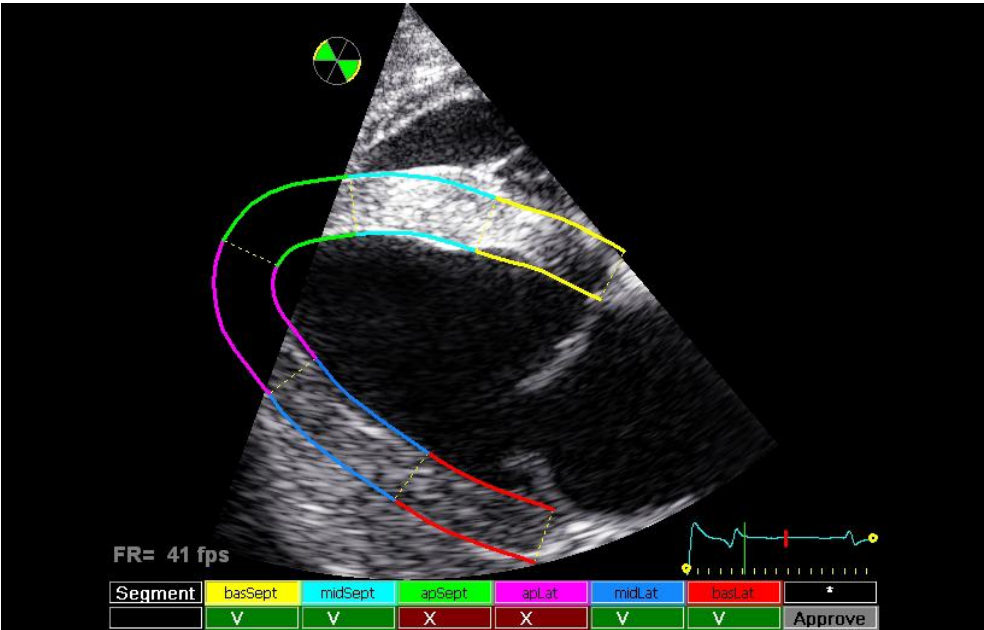
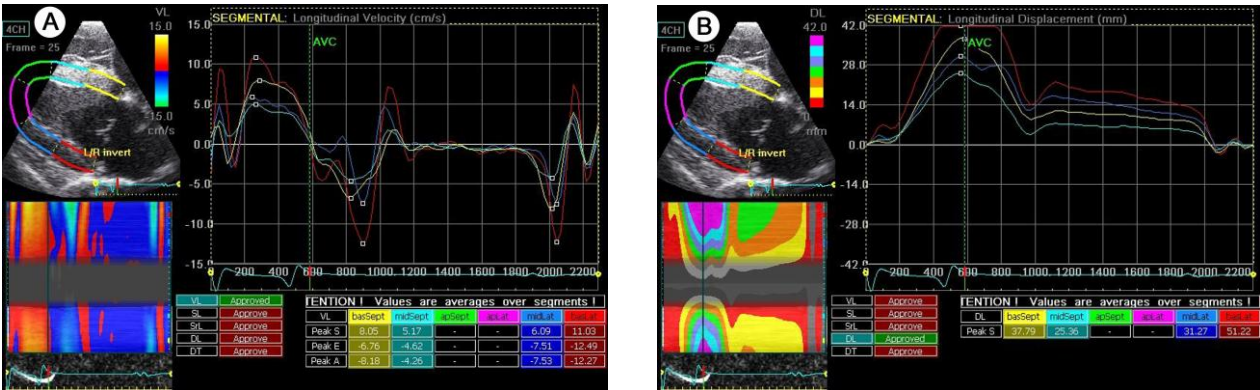


Figure 2A-E: Examples of the curves in the “Results” screen after approval of tracking quality. On the left, a 2D greyscale image is displayed showing the tracked ROI. A parametric color-coded M-mode is depicted below. On the right, the segmental traces are displayed. The vertical axis represents values of the selected variable; the horizontal axis shows time (ms) and the ECG. AVCa is marked by a vertical green line. Peak values are automatically indicated on the curves and tabulated below. After verifying the correct position of these peaks, measurements can be approved in the column next to the table. **A**, VL: longitudinal velocity. **B**, DL: longitudinal displacement. **C**, SL: longitudinal strain. **D**, SrL: longitudinal strain rate. **E**, DT: transverse displacement.



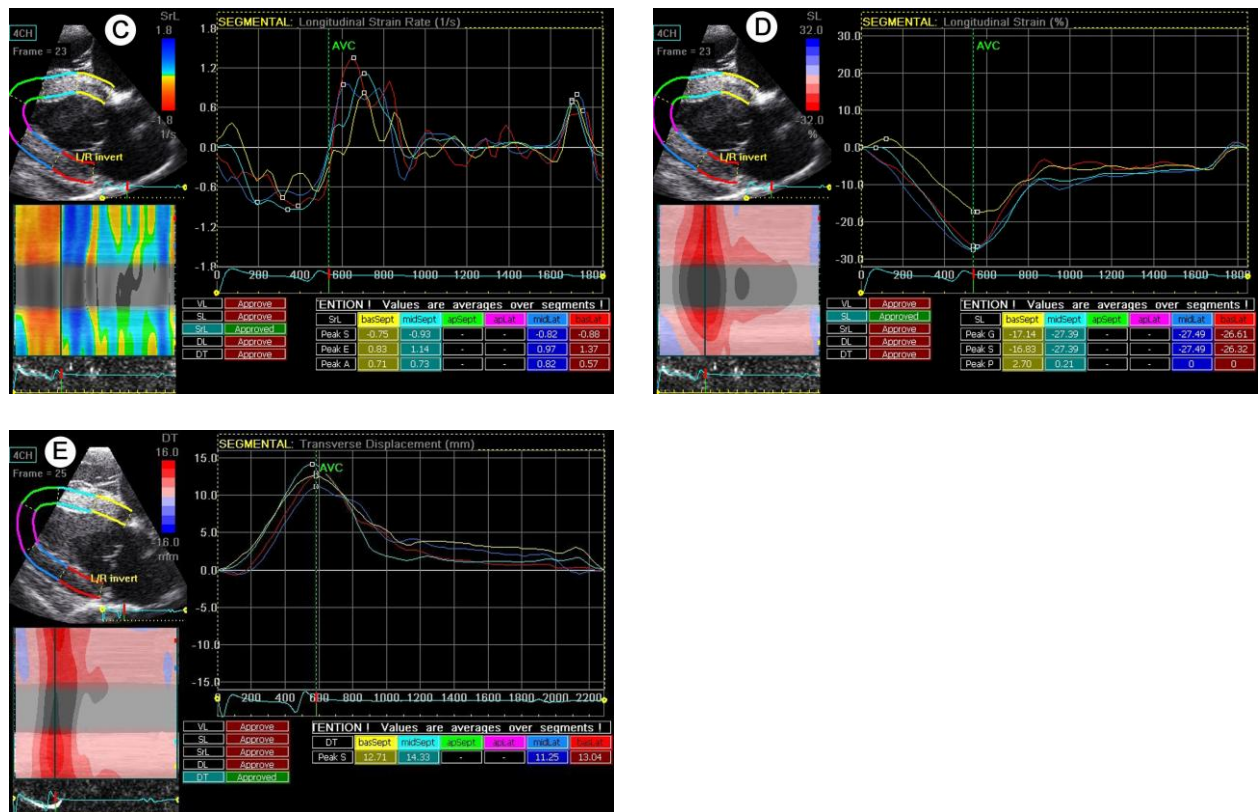
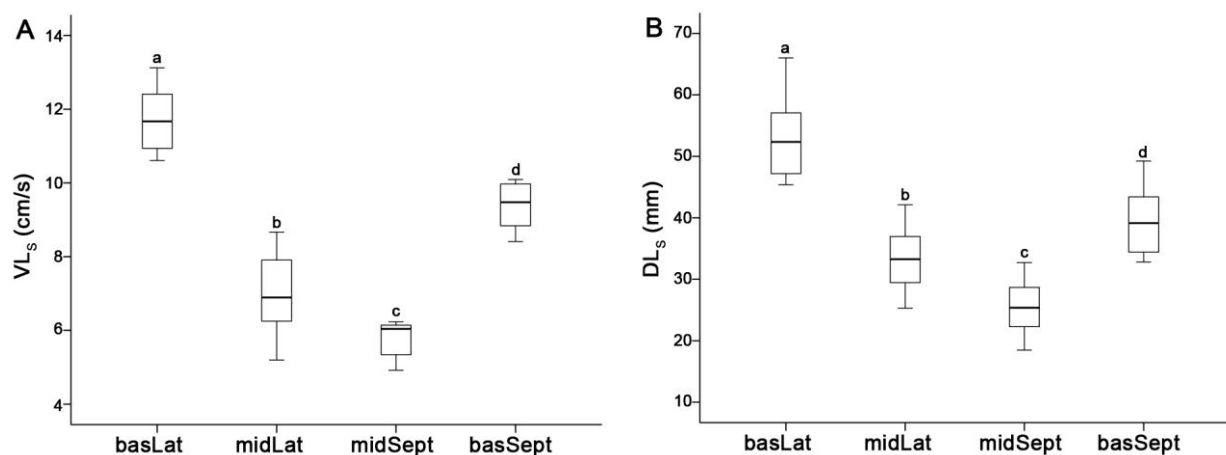


Figure 3A-F: Graphical illustration of segmental differences of 2DST measurements of LV longitudinal function. For each segment, the median and spread of the peak value or timing is indicated by a boxplot, based on the averaged measurement values for each horse ($n = 10$). Boxes marked with different letters are significantly different from each other. **A**, VL_S: peak systolic longitudinal velocity (cm/s). **B**, DL_S: peak systolic longitudinal displacement (mm). **C**, SrL_S: peak systolic longitudinal strain rate (s^{-1}). **D**, SL_G: peak maximal longitudinal strain (%). **E**, time to SL_G (ms). **F**, time to SrL_A: time to peak late diastolic longitudinal strain rate (ms).



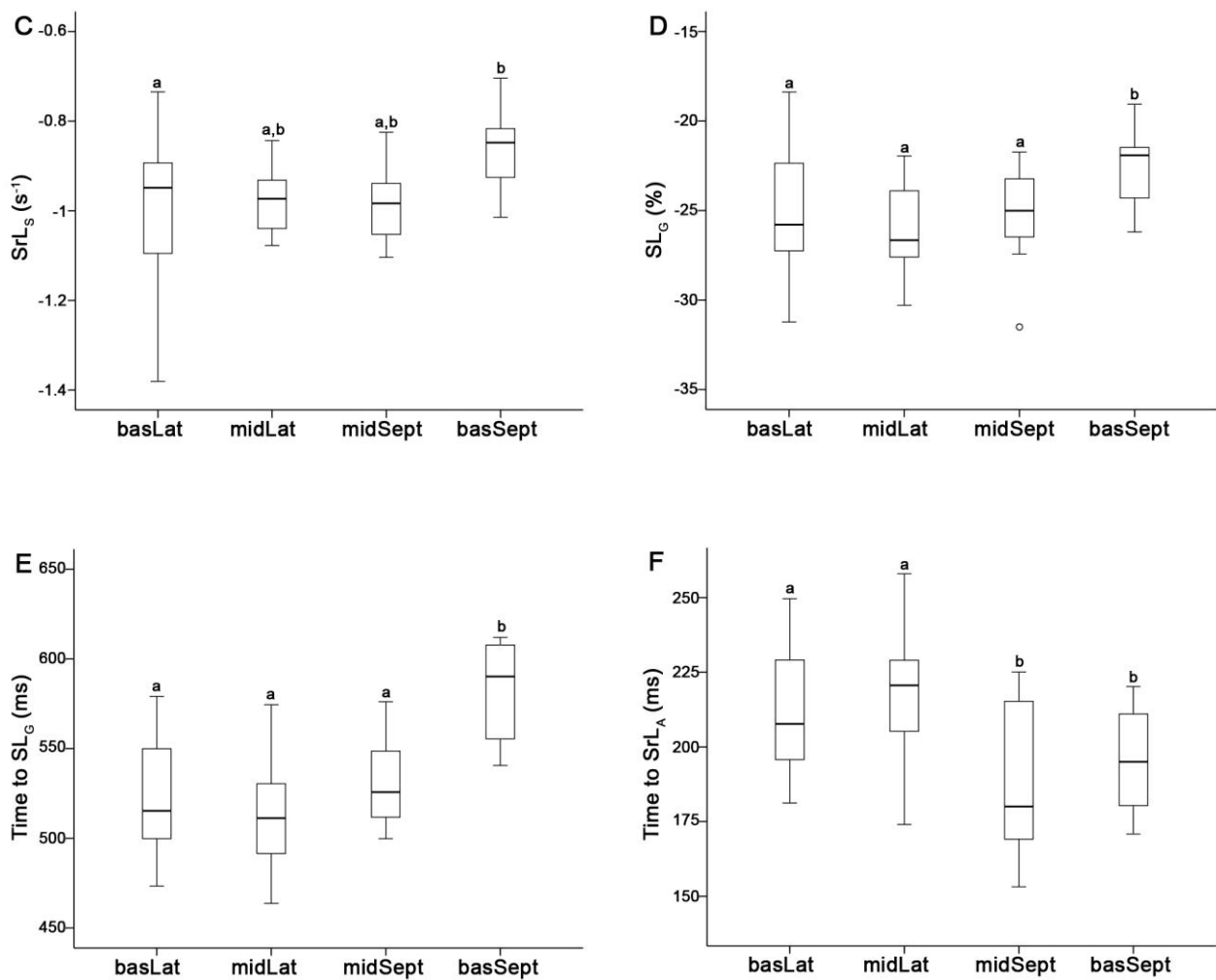


Table 1: Global^a values of 2DST measurements of LV longitudinal function in 10 healthy adult trotter horses.

Variable	Mean	SD	Intra-observer measurement variability CV (%)	Interobserver measurement variability CV (%)	Between-day intra-observer variability CV (%)	Within-day interobserver variability CV (%)
HR (bpm)	33.4	3.88	3.2	3.2	7.7	7.0
AVC _a (ms)	528	26	3.6	3.6	6.1	5.7
SL_G (%)	-24.3	1.72	7.2	7.4	8.3	10.1
SrL_s (s^{-1})	-0.88	0.05	8.9	8.9	8.7	10.9
SrL_E (s^{-1})	0.98	0.09	10.7	9.3	10.8	11.3
SrL_A (s^{-1})	0.63	0.12	14.1	14.5	16.6	20.5

SD = standard deviation. CV = coefficient of variation.

^a Calculated by the software from the whole ROI as a single segment.

Table 2: Segmental and averaged peak values of 2DST measurements of LV longitudinal function in 10 healthy adult trotter horses.

Variable	Segment ^a	n	Mean	SD	Intra-observer measurement variability CV (%)	Interobserver measurement variability CV (%)	Between-day intra-observer variability CV (%)	Within-day interobserver variability CV (%)
SL _G (%)	Avg		-24.80	2.36	7.1	6.5	8.0	11.1
	basLat	139	-25.19	3.83	11.7	13.4	13.7	15.4
	midLat	146	-26.27	2.65	10.2	10.4	12.0	14.1
	midSept	150	-25.36	2.83	6.3	6.2	8.7	9.9
	basSept	139	-22.47	2.15	9.8	8.0	12.7	15.3
SL _S (%)	Avg		-24.49	2.52	7.2	6.5	8.0	11.2
	basLat	139	-25.08	3.84	11.7	13.6	13.7	15.1
	midLat	146	-26.24	2.63	10.2	10.4	12.0	14.2
	midSept	150	-25.23	2.94	6.3	6.2	8.8	9.9
	basSept	139	-21.48	2.28	11.3	9.5	14.3	16.2
SL _P (%)	Avg		1.80	0.49	67.9	57.5	60.9	61.5
	basLat	51	0.98	0.51	61.9	63.9	102.0	154.1
	midLat	17	0.39	0.49	NA	NA	NA	NA
	midSept	86	0.86	0.46	85.2	82.3	124.7	109.8
	basSept	134	2.57	0.76	66.1	73.1	75.4	78.2
VL _S (m/s)	Avg		8.37	0.44	7.6	7.7	10.1	10.1
	basLat	139	11.76	0.88	9.0	7.8	11.4	10.9
	midLat	146	6.96	1.09	16.4	15.7	26.1	26.3
	midSept	150	5.75	0.50	13.3	11.4	14.4	15.0
	basSept	139	9.41	0.61	5.0	6.9	5.9	7.4
VL _E (m/s)	Avg		-7.71	0.50	10.3	10.5	11.9	11.9
	basLat	130	-11.14	0.80	9.3	8.8	13.6	10.0
	midLat	144	-6.17	0.98	20.1	19.7	21.7	20.7
	midSept	128	-5.32	0.45	14.4	11.1	17.5	14.4
	basSept	137	-8.33	1.15	7.9	8.2	11.5	12.3
VL _A (m/s)	Avg		-7.46	0.76	9.0	9.2	11.5	11.7
	basLat	130	-9.68	0.99	15.1	17.1	16.0	15.4
	midLat	144	-6.19	0.95	17.3	18.3	21.2	21.0
	midSept	128	-5.25	0.48	13.1	13.2	13.8	19.1
	basSept	137	-8.52	1.54	7.6	8.3	13.8	15.0
SrL _S (s ⁻¹)	Avg		-0.95	0.08	7.8	7.3	8.6	10.1
	basLat	139	-1.00	0.18	16.3	16.1	16.4	19.0
	midLat	146	-0.97	0.08	10.3	11.5	12.1	11.3
	midSept	150	-0.98	0.09	8.2	8.4	8.5	11.9
	basSept	139	-0.86	0.11	11.7	12.2	15.7	21.6
SrL _E (s ⁻¹)	Avg		1.18	0.10	9.7	8.8	10.4	11.3
	basLat	130	1.51	0.20	19.9	17.0	21.5	24.6

	midLat	144	1.03	0.07	13.7	13.5	14.7	13.6
	midSept	128	1.03	0.11	10.6	10.1	11.0	13.6
	basSept	137	1.19	0.24	16.7	17.0	19.4	21.1
SrL _A (s ⁻¹)	Avg		0.67	0.13	13.5	14.0	15.0	16.1
	basLat	130	0.55	0.15	44.6	41.4	45.9	45.1
	midLat	144	0.76	0.09	19.9	19.9	21.6	23.3
	midSept	128	0.69	0.15	11.8	13.1	16.5	18.8
	basSept	137	0.66	0.20	18.1	23.1	23.7	20.1
DL _S (mm)	Avg		37.60	5.18	12.3	11.2	13.2	15.5
	basLat	139	53.60	6.91	9.6	9.2	11.1	12.9
	midLat	146	33.70	5.50	16.6	15.1	17.7	19.5
	midSept	150	25.60	4.24	18.9	14.3	17.0	18.7
	basSept	139	39.77	5.42	9.9	8.9	11.6	14.2

n = number of segments in which the variable could be determined (on a total of 150). SD = standard deviation. CV = coefficient of variation. NA = not available

^a Segments as illustrated in Fig. 1. Avg = average of the approved segments.

Supplementary Table 1: Segmental and averaged peak timing of 2DST parameters of LV longitudinal function in 10 healthy adult trotter horses.

Variable ^a	Segment ^b	Mean	SD	Acquisition CV (%)			
				Measurement CV (%)			
				Intra-observer	Inter-observer	Between-day	Inter-observer
Time to SL _G (ms)	Averaged	537	23	3.6	3.5	6.1	5.3
	basLat	521	34	4.4	4.1	6.6	6.7
	midLat	516	32	3.2	3.1	4.9	4.7
	midSept	528	24	5.1	5.6	8.0	6.7
	basSept	582	27	6.1	5.3	7.3	6.8
Time to SL _S (ms)	Averaged	518	30	3.0	3.0	5.6	5.0
	basLat	515	32	3.8	3.6	6.0	6.1
	midLat	513	31	3.1	3.0	4.8	4.5
	midSept	517	30	3.0	3.1	6.1	4.9
	basSept	526	28	3.8	3.8	6.4	5.8
Time to SL _P (ms)	Averaged	82	16	38.0	32.8	37.0	36.1
	basLat	45	13	21.6	27.4	42.7	35.0
	midLat	42	39	NA	NA	NA	NA
	midSept	75	26	21.4	18.8	67.2	43.5
	basSept	100	16	27.8	27.6	36.2	38.5
Time to VL _S (ms)	Averaged	234	25	12.8	13.0	17.2	15.0
	basLat	238	37	20.4	20.3	29.1	25.5
	midLat	230	54	23.5	24.8	28.4	27.0
	midSept	227	32	13.8	13.8	17.0	17.9
	basSept	246	32	17.7	14.1	16.7	19.7
Time to VL _E (ms)	Averaged	756	44	3.6	3.6	4.1	4.2
	basLat	746	53	7.5	7.1	7.3	7.6
	midLat	766	53	7.2	7.4	6.2	6.7

	midSept	774	42	3.5	3.4	4.7	4.6
	basSept	742	45	4.2	3.9	5.1	6.3
Time to VL _A ^c (ms)	Averaged	212	23	7.2	7.2	8.9	9.9
	basLat	229	24	8.4	8.5	9.5	10.9
	midLat	227	25	7.4	7.1	9.2	10.9
	midSept	191	25	12.1	11.4	12.2	14.4
	basSept	202	27	8.0	8.1	9.1	11.4
Time to SrL _S (ms)	Averaged	293	48	12.2	12.3	15.2	16.3
	basLat	280	38	32.8	30.9	37.7	31.0
	midLat	270	52	23.0	24.2	33.0	26.6
	midSept	293	53	23.7	24.8	23.9	27.3
	basSept	336	65	21.7	25.5	25.8	31.8
Time to SrL _E (ms)	Averaged	705	45	3.9	3.6	4.5	5.1
	basLat	673	41	5.0	5.3	7.1	7.0
	midLat	701	63	8.6	9.1	9.6	9.2
	midSept	723	37	3.9	3.7	4.1	5.5
	basSept	722	54	6.1	5.5	6.4	8.3
Time to SrL _A ^c (ms)	Averaged	203	19	8.8	9.3	10.6	12.7
	basLat	214	22	18.1	21.7	23.3	23.1
	midLat	220	25	8.2	8.8	10.2	12.5
	midSept	185	25	10.1	9.8	10.3	15.3
	basSept	195	17	9.6	9.7	11.3	15.4
Time to DL _S (ms)	Averaged	501	31	2.7	2.8	5.3	4.0
	basLat	507	31	2.6	2.8	4.6	3.9
	midLat	503	32	3.1	3.0	5.5	3.9
	midSept	491	33	5.2	5.5	7.3	5.4
	basSept	506	31	2.8	2.8	5.3	4.5

SD = standard deviation. CV = coefficient of variation. NA = not available

^a Time to peak measured from R-wave, unless indicated otherwise.

^b Segments as illustrated in Fig. 1. Averaged = average of the approved segments.

^c Time to peak measured from onset P-wave.